

$\rightarrow \pi^0 X$, simply because the π^0 is symmetric in u , \bar{u} , d , and \bar{d} quarks, of which also the initial systems are composed. The only differences of relevance are that there are 50% more quarks in a proton than in a pion (the same is assumed for the sea) and that the pion constituents hence get 50% more kinetic energy than the proton constituents with the same projectile momentum.

Thus I get

$$1.5 \times (\pi^- p \rightarrow \pi^0 X \text{ at } 200 \text{ GeV}/c) \\ = (p p \rightarrow \pi^0 X \text{ at } 300 \text{ GeV}/c). \quad (1)$$

To test this relation in the interval $0 \lesssim x_T \lesssim 0.6$, I rewrite it in the form

$$\frac{(p p \rightarrow \pi^0 X)_{200}}{(\pi^- p \rightarrow \pi^0 X)_{200}} = 1.5 \frac{(p p \rightarrow \pi X)_{200}}{(p p \rightarrow \pi X)_{300}}, \quad (2)$$

where π in the right-hand side means averaging over π^+ and π^- production to estimate π^0 yields. I take the left-hand side directly from Ref. 1 and estimate the right-hand side from the Chicago-Princeton data⁶ on proton-tungsten collisions.

The presence of neutrons in the tungsten target should not bias this test and the A dependences in the cross sections in the right-hand side are presumably divided out.

It can be seen in Fig. 1 that Eq. (2) is remarkably successful in the full x_T range. I therefore conclude that the presence of a leading antiquark in the beam pion seems to be unimportant for π^0 production in the studied p_T interval, in contrast to the simple fact that the projectile has two valence quarks instead of three.

I have benefitted from discussions with L. Bergström. Financial support from the Swedish Atomic Research Council is gratefully acknowledged.

¹G. Donaldson *et al.*, Phys. Rev. Lett. **36**, 1110 (1976).

²R. Blankenbecler, S. J. Brodsky, and J. Gunion, Phys. Rev. D **12**, 3469 (1975).

³B. L. Combridge, Phys. Rev. D **10**, 3849 (1974).

⁴S. J. Brodsky, in SLAC Report No. 191 (unpublished).

⁵S. Fredriksson, Phys. Lett. **63B**, 321 (1976).

⁶J. W. Cronin *et al.*, Phys. Rev. D **11**, 3105 (1975).

Production of High-Mass Muon Pairs in Proton-Nucleus Collisions at 400 GeV

D. C. Hom, L. M. Lederman, H. P. Paar,* H. D. Snyder, J. M. Weiss, and J. K. Yoh
Columbia University, New York, New York 10027†

and

J. A. Appel, B. C. Brown, C. N. Brown, W. R. Innes, and T. Yamanouchi
Fermi National Accelerator Laboratory, Batavia, Illinois 60510‡

and

R. J. Engelmann, R. J. Fisk, H. Jöstlein, D. M. Kaplan, R. D. Kephart, and R. L. McCarthy
State University of New York, Stony Brook, New York 11794†

(Received 24 August 1976)

We report results on the production of muon pairs in the mass range 2.5 to 20 GeV in 400-GeV proton-nucleus collisions. A total of 159 events are observed in the mass range 5.5 to 11 GeV with a cross section which is in agreement with the previous observation of a high-mass dielectron continuum signal in this interval. Details on the production dynamics and comparisons with parton-model predictions are presented. Within limitations of resolution and continuum uncertainty, the dimuon mass spectrum provides no evidence for fine structure above 5 GeV.

We have previously reported the observation of massive ($\gtrsim 3$ GeV) e^+e^- pairs produced in 400-GeV proton-Be collisions at Fermilab.^{1,2} This Letter reports the results of an experiment we have performed to detect muon pairs over the same mass range. The conversion to muons was motivated by the higher data-taking rate made possible by filtering most hadrons. Although this comes with

poorer mass resolution and different backgrounds, we have been able to increase by a factor of 5 the statistical significance of the high-mass data over that in the e^+e^- run.¹

In order to carry out these observations, our two-arm spectrometer (shown in Fig. 1 of Ref. 1) was modified in a number of ways. Five meters of Be were added as a hadron filter just down-

stream of the target in the 50–95 mrad aperture of each arm. This was followed by 1 m of CH_2 . A hodoscope of horizontal scintillators was installed inside each of the spectrometer magnets in order to define muon trajectories better. Two gas Cherenkov counters in each arm provided a high-energy threshold for muons of $\sim 12 \text{ GeV}/c$. Also, an 8-nuclear-mean-free-path hadron calorimeter was installed behind the lead-glass calorimeter to reject hadrons which punch through the hadron filter. Finally, the muon character of the event was insured by the addition of 1.3 m of steel behind each hadron calorimeter, followed by a set of three liquid-scintillator muon counters.

Data were collected with Cu and Be targets of $\sim 30\%$ of an interaction length using a proton beam intensity of $(6-9) \times 10^{10}$ protons per pulse. Backgrounds in the dimuon run arise from several sources: (i) muons from pion and kaon decays which contribute to pairs either by accidental coincidences or by correlations of the parent hadrons, and (ii) low-energy muons which capitalize on the absence of detectors upstream of the magnet and simulate high-momentum muons by Coulomb scattering.

A large component of the background was observed and dealt with by studying $\mu^+\mu^+$ and $\mu^-\mu^-$ pairs. About 30% of the running time was invested in these studies. The same-sign pairs are dominated by accidental coincidences ($70 \pm 30\%$), as monitored by the technique described in Ref. 1. Since it is known from lower-mass meson studies³ that $h^+h^+ + h^-h^- \cong 2h^+h^-$, a straight subtraction of $\frac{1}{2}(\mu^+\mu^+ + \mu^-\mu^-)$ removes background of type (i) above.⁴ Additional background comes from real $\mu^+\mu^-$ pairs at lower mass (e.g., ψ) which, through multiple Coulomb scattering, appear at higher mass. Monte Carlo studies of these effects show that they are negligible above 5 GeV.

Sufficient redundancy in the muon identification was obtained from cuts on track quality χ^2 , the correct hodoscope element inside the magnet, Cherenkov counter pulse heights, the correct muon counter pulse height, and reconstructed horizontal target location.

Cross sections are obtained using a Monte Carlo calculation of the acceptance which includes the effects of the substantial energy loss of muons in the beryllium and CH_2 absorbers including the contributions of Landau straggling and bremsstrahlung. In the energy determination of the muons, the calculation of Sternheimer⁵ for the *most probable* energy loss has been used. Strin-

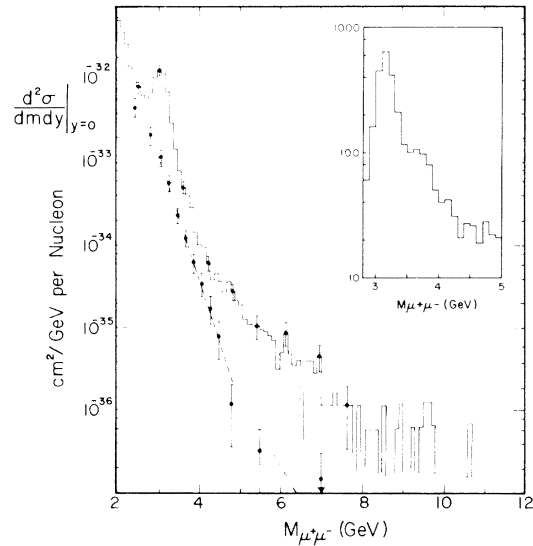


FIG. 1. High-mass dimuon spectrum. Errors are statistical only. Cross sections are in units per nucleon from the Cu target assuming a linear A dependence. Dashed curve is the background obtained from $\frac{1}{2}(\mu^+\mu^+ + \mu^-\mu^-)$. Inset shows the raw data sample in the ψ' region taken with the high-mass spectrometer setting.

gent tests of the Monte Carlo and of this procedure are met by prediction of the observed target distribution and the observed resolution of the J/ψ and of its correctly observed mass value.

The Monte Carlo program calculates an acceptance in the variables m , p_t , y , and $\cos\theta^*$ of the dimuon, where $\cos\theta^*$ is the decay angle in the dimuon rest frame. We note that the acceptance in y is centered near $y \approx 0$ and ranges from -0.2 to $+0.3$ while the mass acceptance is very broad with sensitivity extending out to 20 GeV.

Figure 1 presents the cross section $d^2\sigma/dm dy$ at $y \approx 0$ versus dimuon mass. An inset also shows a sample of raw data. A total of 159 events are observed above a mass of 5.5 GeV with the Cu target; a strong J/ψ peak and a shoulder consistent with ψ' are also noted.² The mass spectrum for $m > 4.5 \text{ GeV}$ is model-independent to the level of $\pm 30\%$ based on the observed distributions of the dynamic variables.⁶ In addition, there is an overall uncertainty of $\pm 40\%$ in the absolute normalization due to uncertainty in flux, efficiency, and A dependence (see below). Our best estimate of the background, obtained from $\frac{1}{2}(\mu^+\mu^+ + \mu^-\mu^-)$, is indicated as the dashed line in Fig. 1.

Figure 2 presents the dynamics of the high-mass dimuons. In Fig. 2(a) we plot the invariant cross section $E d^3\sigma/dp^3$ at $y=0$ versus the transverse momentum, p_t , for each of four mass in-

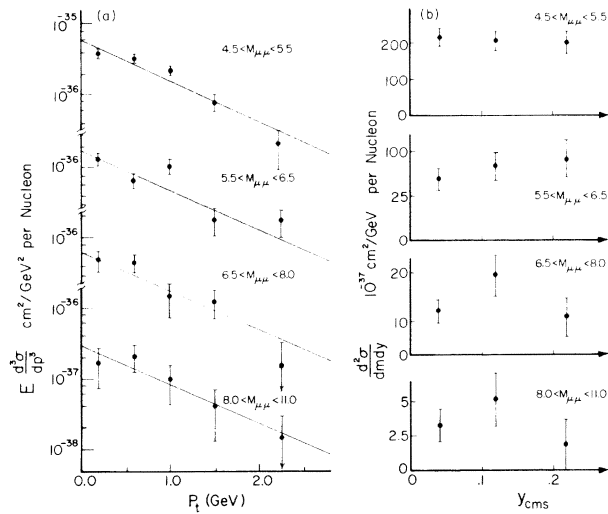


FIG. 2. Dynamics of high-mass dimuons; (a) $E d^3\sigma/dp^3$ at $y \approx 0$ versus p_t for four mass intervals [the solid lines represent $\exp(-1.29p_t)$] and (b) $d^2\sigma/dm dy$ versus $|y|$ for the same mass intervals. Background has not been subtracted.

intervals above 4.5 GeV. As shown by the solid lines in Fig. 2(a), the data can be well fitted by an exponential form $\exp(-bp_t)$ with a mass-independent slope parameter $b = 1.29 \pm 0.10$ GeV. Fitting mass intervals separately gives the slope parameters $b = 1.26 \pm 1.3$, 1.18 ± 0.24 , 1.52 ± 0.28 , and 1.22 ± 0.39 GeV $^{-1}$ for the four mass intervals shown in Fig. 2. The background is less than 10% in each of these mass bins and has not been subtracted from any of the distributions. We note that these p_t distributions are extremely broad ($\langle p_t \rangle \approx 1.5$ GeV/c) and are in fact characteristic of the trend seen in the production of hadrons.⁷

Figure 2(b) gives the dependence of the invariant cross section, integrated over p_t , on the center-of-mass rapidity y for the same four mass intervals. The data in each mass interval show no significant y dependence in our narrow range of acceptance ($-0.2 < y < +0.3$).

The 360 events on Cu observed with $m > 4.5$ GeV give cross sections $d^2\sigma/dm dy$ at $y \approx 0$ in coarse mass intervals which are given in Table I. These background-subtracted cross sections are plotted in Fig. 3, where they are compared with our electron results¹ and with the predictions of the Drell-Yan parton-antiparton annihilation model⁸ employing a variety of parton and antiparton distributions.⁹⁻¹¹

We note further, as in Ref. 1, that all of the parton-model predictions require the additional color degree of freedom in order to be consistent

TABLE I. High-mass dimuon cross section (copper target).

Mass (GeV)	$(d^2\sigma/dm dy)_{y=0}$ (10^{-37} cm 2 /GeV nucleon)
4.5-5.0	264 \pm 26
5.0-5.5	114 \pm 14
5.5-6.0	66.4 \pm 9.8
6.0-6.5	51.2 \pm 7.8
6.5-7.0	30.7 \pm 5.9
7.0-7.5	12.4 \pm 3.7
7.5-8.0	9.1 \pm 3.2
8.0-9.0	4.7 \pm 1.7
9.0-10.0	4.4 \pm 1.7
10.0-11.0	0.7 \pm 0.7
11.0-13.0	< 0.8
13.0-15.0	< 1.5
15.0-20.0	< 2.2

with the data integrated over p_t . The parton model of Ref. 10 with $x\bar{u}(x) \propto (1-x)^7$ for the antiparton distribution seems to characterize the observed mass dependence of the data best although it lies yet a factor of ~ 1.5 higher in normalization.⁶ The effect of the observed broad p_t distributions upon these predictions is not clear to us in these comparisons and arises fundamental questions about the limitations of the Drell-Yan model.¹²

The measured cross section $(d^2\sigma/dm dy)_{y=0}$ can

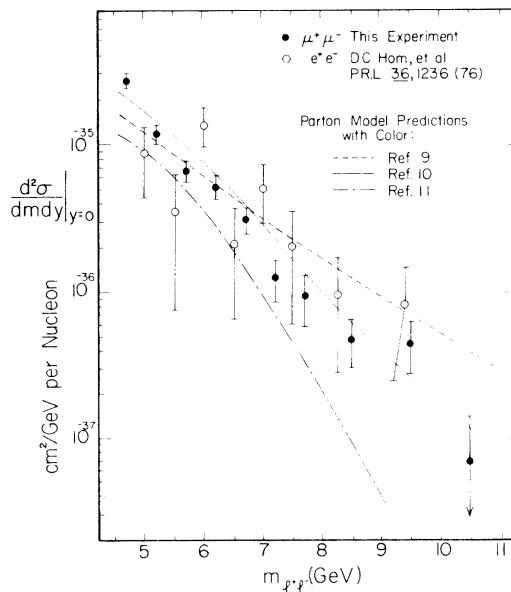


FIG. 3. High-mass dilepton production at 400 GeV. All data are background-subtracted and errors are statistical only.

be simply parametrized in the scaling form:

$$m^3 \left(\frac{d^2\sigma}{dm dy} \right)_{y=0} = (3.8 \pm 1.4) \times 10^{-32} \\ \times e^{-(15.7 \pm 1.6)\sqrt{\tau}} \text{ cm}^2 \text{ GeV}^2,$$

where $\tau = m^2/s$. This predicts an increase in cross section of a factor of 15 at $m = 10$ GeV for a c.m. energy of $\sqrt{s} = 52$ GeV and it also predicts a cross section greater than 7×10^{-35} cm² for production of a W^\pm (with $m = 100$ GeV) at $\sqrt{s} = 400$ GeV.¹³

A separate sample of data with a beryllium target contains 31 events with $m > 5.5$ GeV and, in conjunction with the Cu data, determines the A dependence in that mass range to be $A^{0.95 \pm 0.15}$. All cross sections reported here are in units per nucleon under the assumption of a purely linear A dependence at all masses.

The search for fine structure in a dimuon experiment is hindered by the poor mass resolution ($\pm 2.7\%$ rms) relative to dielectrons. The data do not confirm a possible structure suggested by a clustering of twelve dielectron events near $m_{e^+e^-} = 6.0$ GeV in the previous experiment.^{1,14} We have established (at 95% confidence level) the upper limit on the cross section for a narrow resonance (i.e., less than the resolution of 380 MeV full width at half-maximum at 6 GeV) which can be accommodated by the data to be $(d\sigma/dy)_{y=0} B = (1.3 - 2.7) \times 10^{-36}$ cm², depending upon assumptions about the continuum shape. This value is only $\frac{1}{4}$ to $\frac{1}{2}$ of the cross section represented by the clustering in the dielectron experiment. We note that the discrepancy with the e^+e^- data could have three origins: (i) The electron data are a "one-in-fifty" statistical fluctuation; (ii) the normalization, A dependence, and resolution differences conspire to obscure the signal in the dimuon data; and (iii) least likely, an apparent μ - e difference is being observed. In forthcoming runs, we hope to double the dielectron data and to increase the muon data by an order of magnitude, while improving the latter resolution by a factor of 1.5.

In summary, we have confirmed our previous observation of a massive dilepton signal above 5 GeV with better statistics and more information on the production dynamics of the continuum signal. In as much detail as we can measure, the data are in gross agreement with a color-added parton model except for the unexpected broad-transverse-momentum behavior.

We gratefully acknowledge the support of the Fermilab Proton Laboratory and of P. A. Bury, H. Cunitz, M. L. Good, K. Gray, K. Kephart,

P. P. Lucey, R. Meyers, F. H. Pearsall, T. Regan, B. Tews, W. Sippach, S. J. Upton, and H. Wahl.

*Present address: CERN, 1211 Geneva 23, Switzerland.

†Research supported by the National Science Foundation.

‡Research supported by the U. S. Energy Research and Development Administration.

¹D. C. Hom *et al.*, Phys. Rev. Lett. **36**, 1236 (1976).

²H. D. Snyder *et al.*, Phys. Rev. Lett. **36**, 1415 (1976).

³D. Bintinger *et al.*, Phys. Rev. Lett. **37**, 732 (1976).

To the extent that accidentals dominate the background the subtraction method is good to $\leq 10\%$ of itself. For correlated hadrons, the relation at lower masses is good to 10%.

⁴We note that this procedure also subtracts any real same-sign signal whose source could give rise to real $\mu^+\mu^-$ pairs. Since the subtraction itself is small, the effect is not important.

⁵R. M. Sternheimer and R. F. Peierls, Phys. Rev. B **11**, 3681 (1971); R. M. Sternheimer, Phys. Rev. **115**, 137 (1959).

⁶Results are reported assuming an isotropic decay distribution. However, a $1 + \cos^2\theta^*$ distribution in the Gottfried-Jackson frame would raise all cross sections at high mass by 1.28 while $\sin^2\theta^*$ would reduce them by 0.69. This constitutes the dominant model-dependent uncertainty in the cross sections reported.

⁷Authors who have considered the transverse-momentum distributions in the parton model predict a $(m_c^2 + p_t^2)^{-4}$ dependence which is consistent with our data for $m_c^2 \approx 4$. See, for example, M. Duongvan, SLAC Report No. SLAC-PUB-1604, 1975 (unpublished); J. F. Gunion, Phys. Rev. D **14**, 1400 (1976).

⁸S. D. Drell and T. M. Yan, Phys. Rev. Lett. **25**, 316 (1970).

⁹L. L. Wang, private communication; S. Pakvasa, D. Parasher, and S. F. Tuan, Phys. Rev. Lett. **33**, 112 (1974).

¹⁰G. R. Farrar, Nucl. Phys. **B77**, 429 (1974); J. F. Gunion, Phys. Rev. D **10**, 242 (1974).

¹¹H. P. Paar and E. A. Paschos, Phys. Rev. D **10**, 1502 (1974); also J. Bjorken (on the "most pessimistic form"), private communication.

¹²Crucial tests of the model involve a demonstration of scaling, a comparison with pion-induced dileptons, and a proof of single parent origin by a study of high-mass μe pairs.

¹³Y. Yamaguchi, Nuovo Cimento **43A**, 193 (1966); L. M. Lederman and B. G. Pope, Phys. Rev. Lett. **27**, 765 (1971).

¹⁴Also see D. Eartley, G. Giacomelli, and K. Pretzl, Phys. Rev. Lett. **36**, 1355 (1976).